Supplementary Materials
Anomalous Anisotropic Exciton Temperature Dependence in Rutile TiO_2

Edoardo Baldini,[1] Adriel Dominguez,[2] Letizia Chiodo,[3] Evgeniia Sheveleva,[4]
Meghdad Yazdi-Rizi,[4] Christian Bernhard,[4] Angel Rubio,[2,5] and Majed Chergui[1]

[1] *Laboratory of Ultrafast Spectroscopy, ISIC and Lausanne Centre for Ultrafast Science (LACUS), École Polytechnique Fédérale de Lausanne, CH-1015 Lausanne, Switzerland*
[2] *Max Planck Institute for the Structure and Dynamics of Matter, Hamburg, Germany*
[3] *Unit of Nonlinear Physics and Mathematical Modeling, Department of Engineering, Università Campus Bio-Medico di Roma, Via Álvaro del Portillo 21, I-00128, Rome, Italy*
[4] *Department of Physics, University of Fribourg, Chemin du Musée 3, CH-1700 Fribourg, Switzerland*
[5] *Departamento Física de Materiales, Universidad del País Vasco, Av. Tolosa 72, E-20018, San Sebastián, Spain*

(Dated: July 6, 2017)

I. SPECTROSCOPIC ELLIPSOMETRY

We used spectroscopic ellipsometry (SE) to measure the complex dielectric function of the sample, covering the spectral range from 1.50 eV to 6.50 eV. The measurements were performed using a Woollam VASE ellipsometer. Rutile TiO_2 single crystals were purchased from MTI Corporation, characterized by x-ray Laue diffraction and polished down to optical grade on their (010) surface. Subsequently, the samples were mounted in a helium flow cryostat, allowing measurements from room temperature (T) down to 10 K. The T-dependent measurements were performed at $<10^{-8}$ mbar to prevent measurable ice-condensation onto the sample. Anisotropy corrections were performed using standard numerical procedures [1].

II. *AB INITIO* CALCULATIONS

Many-body perturbation theory at the level of the GW and the Bethe-Salpeter Equation (BSE) [2–4], as implemented within the BerkeleyGW package [5], was employed to compute the band structure and the dielectric response of pristine rutile TiO_2, on top of eigenvalues and eigenfunctions obtained from Density-Functional Theory (DFT). We used the planewave pseudopotential implementation of DFT as provided by the package Quantum Espresso [6]. The DFT calculations were performed using the generalized gradient approximation (GGA) as in the Perdew-Burke-Ernzerhof (PBE) scheme for the exchange-correlation functional. For these calculations, we used normconserving pseudopotentials [7] including semicore states $3s$ and $3p$ (as in Ref. [8] for anatase TiO_2). We used a cutoff of 200 Ry to achieve convergence of the electronic and optical properties at the many body level. A coarse grid of $5 \times 5 \times 7$ k-points was used for PBE and subsequent GW calculations. A more dense, randomly shifted, grid of $16\times16 \times20$ (with interpolation of GW energies on the $5\times5\times7$ grid) was implemented for solving the BSE using Haydock method, to obtain the absorption spectra. The diagonalization of excitonic Hamiltonian was done on a randomly shifted fine grid of $10\times10\times14$ k-points. Such diagonalization provides the analysis of Kohn-Sham orbital contributions and k-points contributions to excitonic wavefunctions. The excitonic wavefunctions in three dimensions were also obtained via direct diagonalization. We used 2498 conduction bands (CBs) and an energy cutoff of 46 Ry for polarisability and inverse dielectric matrix, 2498 CBs for self-energy evaluation, a cutoff energy of 50 Ry and 200 Ry for screened and bare components of self-energy operator, respectively. The 10 topmost valence bands (VBs)nd the 10 lowest CBs were included in the BSE solution via Haydock, while the 7 topmost VBs and the 6 lowest CBs were used for directly diagonalizing BSE Hamiltonian for the excitons analysis.

Our study goes beyond previous experimental/computational works on rutile TiO_2 [9–12] in that: i) a higher computational convergence is achieved; ii) a precise identification and characterization of the peaks in the optical absorption spectrum is made; iii) the T = 0 calculations can be compared with the low-T dielectric function of the material, measured directly via SE and not extracted through a Kramers-Kronig analysis; iv) T effects are included and discussed.

As far as the T = 0 calculations are concerned, the GW indirect bandgap (Γ-R) and direct bandgap (Γ-Γ) are 3.30 eV and 3.34 eV, respectively. These values are converged up to 5 meV and are in good agreement with photoemission and inverse-photoemission results [13]. The present highly-converged value is lower than the gap given in Ref. [9], where a smaller number of bands and k-points was used. The excitonic energies were subsequently obtained by diagonalizing the excitonic Hamiltonian. The first eigenvalue for both light polarizations correspond to a dark triplet exciton with energy 3.19 eV. This dark exciton has a major contribution from the transitions from the VB to the CB at the Γ point. Its binding energy is estimated $\sim$ 150 meV. The large excitonic peak, for light polarized along the a-axis,

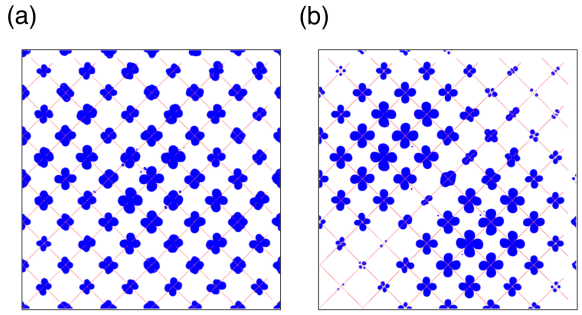

FIG. S1. Wavefunctions of the fundamental charge excitations in rutile TiO_2. Isosurface representation of the electronic configuration on the (001) plane when the hole of the considered excitonic pair is localized close to one oxygen atom. The coloured region represents the excitonic squared modulus wavefunction. (a) Resonant exciton I at 3.99 eV. (b) Resonant exciton IV at 4.24 eV.

at 3.99 eV is composed of various eigenvalues with reciprocal space contributions from a broad region around Γ. This is a resonant, non-bound exciton. For light polarized along the c-axis, the intense and broad excitonic peak centered at 4.24 eV is composed of various eigenvalues, with reciprocal space contributions from a wider region around the Γ point and strong contributions from points close to Γ along the Γ-Z line. Also this peak is a resonant non-bound exciton, retaining a bulk delocalized character. The excitonic wavefunctions on the (001) plane are represented in Fig. S1(a,b). The isosurface represents the electronic part of the excitonic squared modulus wavefunction, with the hole fixed at a site close to one oxygen atom.

To include the T-effects on the electronic and optical properties of rutile TiO_2, we estimated the role of the deformation potential coupling by performing frozen phonon GW-BSE calculations. We separately displaced the ions in the primitive unit cell according to the eigenvector of the longitudinal optical (LO) $E_u^{(3)}$ and A_{2u} modes [14]. These phonons are expected to possess the strongest coupling with the electronic degrees of freedom along the a-axis of the crystal [15, 16]. The displacement of atom j was calculated from the harmonic oscillator mean square displacement at 250 K according to

$$< |u_j(t)|^2 >= \frac{\hbar(1+2n_{BE})}{2m_j\omega} \quad (1)$$

where $n_{BE} = (e^{\hbar\omega/k_BT} - 1)^{-1}$ is the Bose-Einstein statistical occupation factor, k_B is the Boltzmann constant, m_j is the atomic mass and ω is the phonon frequency. We corrected the GW gap values for the lattice expansion effect by using the thermal expansion coefficient reported in Ref. [17]. In particular, the a and c lattice parameters of rutile TiO_2 increase by 0.3 % from 0 to 250 K. The inclusion of both the phonon-induced and the thermal expansion-induced effects leads to a net blueshift of the bandgap of $\sim$ 120 meV (in the case of the $E_u^{(3)}$ mode) and 60 meV (in the case of the A_{2u} mode). A similar trend was recently reported in the case of the electronic gap (evaluated within the thermal lines method for electron-phonon coupling), which shows a non-monotonic behaviour with T [18]. When solving the BSE on top of the T-corrected GW results, we find that, in the case of the $E_u^{(3)}$ mode at 250 K, exciton I blueshifts by 190 meV and exciton IV blueshifts by 130 meV. In the case of the A_{2u} mode at 250 K, exciton I blueshifts by 20 meV and exciton IV blueshifts by 60 meV.

III. FRÖHLICH INTERACTION

In polar crystals, a major contribution to the electron-phonon interaction comes from the polarization of the lattice produced by the polar LO modes. The polarization in a unit cell, $\mathbf{p}$, can be written as

$$\mathbf{p} = e^*(\mathbf{R}_1 - \mathbf{R}_2) \quad (2)$$

where $\mathbf{R}_1$ and $\mathbf{R}_2$ are the displacements of the positive and negative ions, respectively, and e^* is the effective charge of the ions, which differs from the fundamental charge e by the effect of the polarization of the ions as a result of their displacements. The structure of the polar electron-phonon interaction has been described by the theory of Fröhlich [19]. The momentum-dependent matrix element of the interaction potential reads

$$\mathscr{M}(q) = \frac{1}{\sqrt{MN}} \frac{2\pi e e^*}{a^3 q} \sqrt{\frac{\hbar}{2\omega_{LO,q}}} \sqrt{n_{BE}+1} \quad (3)$$

where $M = M_1M_2/(M_1+M_2)$ is the reduced mass, N is the total number of unit cells in the lattice, a is the lattice constant (assuming a cubic crystal), $\omega_{LO,q}$ is the frequency of the LO modes at a given momentum q and n_{BE} is the statistical Bose-Einstein occupation factor.

The frequency of a LO mode is approximately constant as a function of q and it is related to the transverse optical (TO) mode frequency ω_{TO} via the Lyddane-Sachs-Teller relationship [20]

$$\omega_{LO}^2 = \omega_{TO}^2(\epsilon_0/\epsilon_\infty) \quad (4)$$

where ϵ_0 and ϵ_∞ are the dielectric constants at energies well below and above the phonon range, respectively. The frequency ω_{TO} itself is related to ϵ_0 and ϵ_∞ by

$$\omega_{TO}^2 = 2\pi e^{*2}\epsilon_\infty/Ma^3(\epsilon_0 - \epsilon_\infty) \quad (5)$$

The energy shift of a charge excitation induced by the Fröhlich interaction is

$$\Delta E_{exc} = -A\left(\frac{1}{\epsilon_\infty} - \frac{1}{\epsilon_0}\right)(1+2n_{BE}) \quad (6)$$

where A is a nearly T-independent prefactor that reads

$$A = e^2\sqrt{\hbar\omega_{\rm LO}}\epsilon_\infty\left(\frac{\sqrt{2m_e^*}}{\hbar}+\frac{\sqrt{2m_h^*}}{\hbar}\right) \qquad (7)$$

where $m_{\rm e}^*$ ($m_{\rm h}^*$) is the electron (hole) effective mass. In this work, we evaluated this formula along the a- and c-axis of rutile TiO_2, accounting for all polar LO modes in the crystal and relying on the experimental values of ϵ_0 and ϵ_∞. The values of $m_{\rm e}^*$ and $m_{\rm h}^*$ were estimated from our *ab initio* calculations, by performing a parabolic fit at the Γ point of the bands involved in the transitions I and IV (see Section II. B). Along the Γ-X line of the Brillouin zone, we obtain $m_{\rm e}^* = 0.61\ m_{\rm e}$ and $m_{\rm h}^* = 1.33\ m_{\rm e}$. Along the Γ-Z line of the Brillouin zone, we obtain $m_{\rm e}^* = 0.73\ m_{\rm e}$ and $m_{\rm h}^* = 5.20\ m_{\rm e}$. Substituting all values in Eq. (6) yields a blueshift of 86 meV for exciton I and of 160 meV for exciton IV. Therefore, the Fröhlich interaction affects the fundamental charge excitations of rutile TiO_2, causing their hardening for increasing T. Indeed, the T dependence of the charge excitations is encoded in the T variation of ϵ_0.

IV. SOFTENING OF EXCITON IV

While the T dependence experienced by all in-plane charge excitations of rutile TiO_2 is anomalous compared to standard semiconductors and insulators, the behaviour of exciton IV is instead conventional. Indeed, in the experimental data, the energy of charge excitation IV undergoes a sizeable softening for increasing T, similarly to the dependence shown by silicon, germanium and other band semiconductors. From our theoretical calculations (see Sections II and III), we highlighted the effect produced by the DP coupling and the Fröhlich interaction on exciton IV, observing a non-negligible hardening of the peak for increasing T. In rutile TiO_2, the effect of thermal expansion is not sufficient to explain the origin of the peak softening, since it is not strong enough to counterbalance the DP and Fröhlich interactions. This implies that other terms in the electron-phonon interaction Hamiltonian are at the origin of the exciton IV softening.

In the following, we describe the conventional redshift experienced by exciton IV by fitting the experimental T dependence with an approximated model. Although this represents a phenomenological approach, this is the most advanced model employed in literature other than *ab initio* treatments. The most general approach uses a distribution of phonon energies to describe the impact of the electron-phonon interaction on the energy ($E_{\rm exc}$) of a charge excitation (i.e. interband transition or excitonic transition) [21]. The shift of $E_{\rm exc}(T)$ can be described

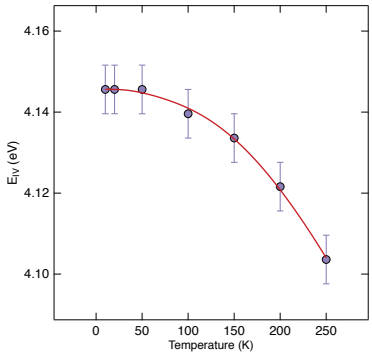

FIG. S2. Temperature behaviour of the peak energy for exciton IV: experimental data are represented as violet dots, the fit is shown as a red curve.

by

$$E_{\rm exc}(T) = E_0 - \int d\omega f(\omega)\Big[n_{\rm BE}(\omega,T)+\frac{1}{2}\Big] - E_{\rm th}(T) \quad (8)$$

where E_0 is the bare (unrenormalized) excitation energy at zero T, $n_{\rm BE}$ is the Bose-Einstein statistical factor ($e^{\hbar\omega/k_{\rm B}T}$ - 1)$^{-1}$, f(ω) is a weighting factor and the last term $E_{\rm th}(T)$ accounts for the lattice thermal expansion. The weighting factor f(ω) can be decomposed into a product of the phonon density of states (PDOS) $\rho(\omega)$ and a factor related to the EPI strength. For an isotropic crystal, the T dependent lattice expansion is given by

$$E_{\rm th}(T) = -3B\left(\frac{\partial E_{\rm exc}}{\partial p}\right)_T\int_0^T \alpha(T')dT' \qquad (9)$$

with α(T) = L$^{-1}(\partial$L/∂T)$_p$, being the linear thermal expansion coefficient, B the bulk modulus and $(\partial E_g/\partial p)_T$ is the dependence of $E_{\rm exc}$ on hydrostatic pressure.

Although representing the most complete approach, Eq. (8) necessitates detailed knowledge of the PDOS and the coupling constants. Moreover, it requires significant computational efforts, making this general treatment rather expensive. This approach can be simplified when the PDOS is dominated by specific peaks due to van Hove singularities in the dispersion relation [22]. For example, along the c-axis, the PDOS of rutile TiO_2 is characterized by the presence of a peak at 12 meV (98 cm^{-1}) due to transverse acoustic (TA) phonons and a peak at 58 meV (467 cm^{-1}) due to the branches of the $E_{\rm g}$ and $E_{\rm u}^{(2)}$ phonons [23]. As such, the PDOS $\rho(\omega)$ can be approximated by two delta-functions positioned at average TA and LO frequencies

$$\rho(\omega) = \delta(\omega-\omega_{\rm TA}) + \delta(\omega-\omega_{\rm LO}) \qquad (10)$$

We assume that the coupling constant for TA phonons is proportional to q^2 whereas for LO phonons is independent of q. Then, the T dependence of $E_{\rm exc}(T)$ can be

written as

$$E_{\rm exc}(T) \approx E_0 - \sum_{i=1}^{2} A_i \omega_{\rm i} (2n_{BE}+1) + E_{\rm th}(T) \qquad (11)$$

where $\omega_1 = \omega_{\rm TA}$ and $\omega_2 = \omega_{\rm LO}$. In the fit, the coupling constants $A_{\rm i}$ are allowed to change sign and magnitude. Conversely, the phonon frequencies $\omega_{\rm i}$ are maintained fixed. Moreover, the lattice expansion term $E_{\rm th}(T)$ is generalized to the case of an anisotropic (tetragonal) crystal, using the expressions for the linear thermal expansion coefficients of rutile TiO_2 as in Ref. [17]. The value of the bulk modulus is taken from Ref. [24], while the dependence of on hydrostatic pressure is extracted from Ref. [25]. The results of the fit are shown in Fig. S2 as a red curve. We observe that the fit reproduces the experimental T dependence in an excellent way. Importantly, we also underline that our fit is robust with respect to the number of Bose-Einstein oscillators used and the choice of the phonon energies at 12 meV and 58 meV. Indeed, the use of different phonon energies other than 12 meV and 58 meV worsen the fit significantly. This proves that the modes playing the major role in the T renormalization of exciton IV are those displaying the strongest peaks in the c-axis PDOS. Furthermore, from the fit, we obtain two very interesting and consistent results: i) the bare excitation energy at zero T (E_0) is found at 4.32 eV, which is 170 meV larger than the experimental excitation energy at 10 K. As such, this value is in very good agreement with the zero-point renormalization of 150 meV calculated in a recent *ab initio* study of the single-particle excitation spectrum of rutile TiO_2 [18]; ii) the modes at 58 meV have a coupling that is by about a factor of 5.5 larger than the one of the 12 meV phonons. This indicates that the effect of the high-energy LO phonons on the T dependence of exciton IV is more important than that of the low-energy TA phonons, in accordance with the relative ratio of the peak heights ($A_{\rm LO}/A_{\rm TO} \sim 5.8$) in the calculated c-axis PDOS. Despite the excellent parameters retrieved from our fit, we remark that this phenomenological approach neglects the detailed q-dependence of the electron-phonon coupling strength. However, prior to our computational study, this approximate model represented one of the most advanced treatments presented in literature.

[1] D. E. Aspnes, JOSA **70**, 1275 (1980).
[2] L. Hedin, Phys. Rev. **139**, A796 (1965).
[3] L. Hedin and S. Lundqvist, *Solid State Physics Vol. 23, 7* (Acadernic Press, New York, 1968).
[4] G. Onida, L. Reining, and A. Rubio, Rev. Mod. Phys. **74**, 601 (2002).
[5] J. Deslippe, G. Samsonidze, D. A. Strubbe, M. Jain, M. L. Cohen, and S. G. Louie, Comput. Phys. Commun. **183**, 1269 (2012).
[6] P. Giannozzi, S. Baroni, N. Bonini, M. Calandra, R. Car, C. Cavazzoni, D. Ceresoli, G. L. Chiarotti, M. Cococcioni, I. Dabo, *et al.*, Journal of physics: Condensed matter **21**, 395502 (2009).
[7] A. M. Rappe, K. M. Rabe, E. Kaxiras, and J. D. Joannopoulos, Phys. Rev. B **41**, 1227 (1990).
[8] E. Baldini, L. Chiodo, A. Dominguez, M. Palummo, S. Moser, M. Yazdi-Rizi, G. Auböck, B. P. P. Mallett, H. Berger, A. Magrez, C. Bernhard, M. Grioni, A. Rubio, and M. Chergui, Nature Communications **8** (2017).
[9] L. Chiodo, J. M. García-Lastra, A. Iacomino, S. Ossicini, J. Zhao, H. Petek, and A. Rubio, Phys. Rev. B **82**, 045207 (2010).
[10] W. Kang and M. S. Hybertsen, Phys. Rev. B **82**, 085203 (2010).
[11] M. Landmann, E. Rauls, and W. Schmidt, J. Phys. Conden. Matt. **24**, 195503 (2012).
[12] H. Lawler, J. Rehr, F. Vila, S. Dalosto, E. Shirley, and Z. Levine, Phys. Rev. B **78**, 205108 (2008).
[13] Y. Tezuka, S. Shin, T. Ishii, T. Ejima, S. Suzuki, and S. Sato, J. Phys. Soc. Jpn. **63**, 347 (1994).
[14] J. G. Traylor, H. Smith, R. Nicklow, and M. Wilkinson, Phys. Rev. B **3**, 3457 (1971).
[15] N. A. Deskins and M. Dupuis, Phys. Rev. B **75**, 195212 (2007).
[16] S. Moser, L. Moreschini, J. Jaćimović, O. Barišić, H. Berger, A. Magrez, Y. Chang, K. Kim, A. Bostwick, E. Rotenberg, *et al.*, Phys. Rev. Lett. **110**, 196403 (2013).
[17] K. K. Rao, S. N. Naidu, and L. Iyengar, J. Amer. Ceram. Soc. **53**, 124 (1970).
[18] B. Monserrat, Phys. Rev. B **93**, 100301 (2016).
[19] H. Fröhlich, H. Pelzer, and S. Zienau, The London, Edinburgh, and Dublin Philosophical Magazine and Journal of Science **41**, 221 (1950).
[20] R. Lyddane, R. Sachs, and E. Teller, Physical Review **59**, 673 (1941).
[21] A. Collins, S. Lawson, G. Davies, and H. Kanda, Phys. Rev. Lett. **65**, 891 (1990).
[22] M. Cardona and R. Kremer, Thin Solid Films **571**, 680 (2014).
[23] R. Sikora, J. Phys. Chem. Sol. **66**, 1069 (2005).
[24] M. H. Manghnani, Journal of Geophysical Research **74**, 4317 (1969).
[25] W.-J. Yin, S. Chen, J.-H. Yang, X.-G. Gong, Y. Yan, and S.-H. Wei, Applied physics letters **96**, 221901 (2010).